

Adsorption of Alkyltrimethylammonium Bromides on Negatively Charged Alumina

Aixing Fan, P. Somasundaran, and Nicholas J. Turro*

Langmuir Center for Colloids and Interfaces, Columbia University,
New York, New York 10027

Received July 22, 1996. In Final Form: November 12, 1996[®]

A four-region model based on electrostatic and hydrophobic interactions adequately explains adsorption of anionic surfactants on positively charged solids such as alumina. In this study, cationic surfactants were used instead for adsorption on negatively charged alumina at pH 10 and at a constant ionic strength of 0.03 M NaCl. In this case, only three distinct regions were observed in the adsorption isotherms and there seemed to be a lack of adsorption region III. In order to elucidate the adsorption mechanisms involved, the electronic spin resonance and fluorescence techniques were used along with vacuum flotation technique. The results suggest that adsorption region III may still exist; the difficulty in detecting it from the adsorption isotherm is probably the result of similar slopes for regions II and III. And this may be attributed to the loose and interpenetrating solloid structure in the case of the cationic amine/negatively charged alumina system. This possibility is discussed with the help of the results of the spectroscopic and flotation studies.

1. Introduction

Adsorption of ionic surfactants on charged metal oxides is a topic of great industrial and academic interest, and this has led to a large number of studies with different models proposed.^{1,2}

The reverse orientation model suggested by Somasundaran *et al.*³ has been particularly successful in describing anionic surfactant adsorption on alumina³ and rutile.^{4,5} Since the adsorption isotherms of these systems can be divided into four distinct regions when plotted on a log–log scale, this model is termed a four-region model. According to this model (Figure 1), the surfactants adsorb electrostatically as individual ions in region I and associate into hemimicelles in region II of the isotherm. In the hemimicelle, the surfactants are oriented with their charged headgroups toward the solid surface, while the hydrocarbon chains protrude into the aqueous phase, thus forming hydrophobic patches on the surface. Further adsorption results in an increasing number of surfactant aggregates, with molecules adsorbing in an opposite orientation once the surface is neutralized by the oppositely charged surfactant. Adsorption in region III occurs through the growth of aggregates already formed in region II without an increase in the number of aggregates. Finally, in the plateau region, region IV, the adsorbed layer possesses the structure of a bilayer. The four-region model is supported by *in situ* fluorescence, Raman and ESR studies.^{6–10} A slightly different model,

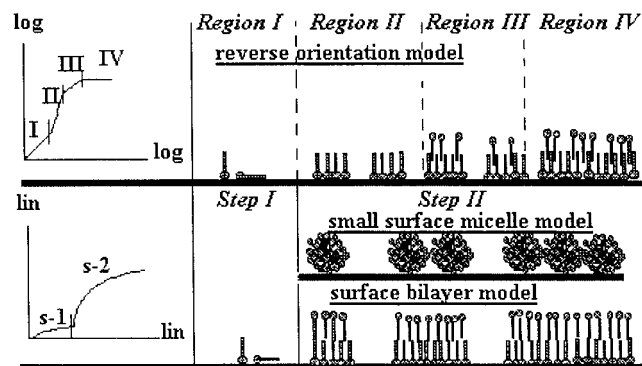


Figure 1. Adsorption isotherms and structures of the surfactant aggregates on solid surfaces according to the reverse orientation model, the (surface) bilayer model, and the small surface micelle model (the *x* axis indicates residual concentrations of surfactants and *y* axis indicates adsorption densities).

the bilayer model, has been presented by Harwell *et al.*^{11,12} (Figure 1). According to this model, local bilayer structures form on patches of the solid surface at a critical solution concentration without hemimicelles at lower surfactant concentrations. These patches of surfactant bilayers were called “admicelles”. Admicelles were proposed to form already in region II. By growing in number and size they will eventually form a more or less complete bilayer.

A much different model was proposed by Gu *et al.*^{13–15} According to this model, the adsorption of the surfactant shows a two-step characteristic, which is evident on a linear scale adsorption isotherm (Figure 1). In the first step, the surface active species are adsorbed through interactions with the solid surface, which is the same as what is proposed for region I in four-region model, and in the second step, they are adsorbed through interactions between the adsorbed surfactants, such that small “surface micelles” are formed. A picture consistent with this model

[®] Abstract published in *Advance ACS Abstracts*, January 15, 1997.

(1) Hough, D. B.; Rendall, H. M. In *Adsorption from Solution at Solid/Liquid Interface*; Parfitt, C. D., Rochester, C. H., Eds.; Academic Press: London/New York, 1983; Chapter 6.

(2) Koopal, L. K. *Surfactant Science Series Vol. 47, coagulation and flocculation: theory and applications*; Dobias, B., Ed.; Dekker: New York, 1993; Chapter 4, p 101.

(3) Somasundaran, P.; Fuerstenau, D. W. *J. Phys. Chem.* **1966**, *70*, 90.

(4) Böhmer, M. R.; Koopal, L. K. *Langmuir* **1992**, *8*, 2649.

(5) Böhmer, M. R.; Koopal, L. K. *Langmuir* **1992**, *8*, 2660.

(6) Chandar, P.; Somasundaran, P.; Waterman, K. C.; Turro, N. J. *J. Colloid Interface Sci.* **1987**, *91*, 148.

(7) Chandar, P.; Somasundaran, P.; Turro, N. J. *J. Colloid Interface Sci.* **1987**, *117*, 31.

(8) Esumi, K.; Nagahama, T.; Meguro, K. *Colloids Surf.* **1991**, *57*, 149.

(9) Esumi, K.; Sugimura, A.; Yamada, T.; Meguro, K. *Colloids Surf.* **1992**, *62*, 249.

(10) Levitz, P.; van Danne, H.; Keravis, D. *J. Phys. Chem.* **1985**, *88*, 2228.

(11) Harwell, J. H.; Hoskins, J. C.; Schechter, R. S.; Wade, W. H. *Langmuir* **1985**, *1*, 251.

(12) Yeskie, M. A.; Harwell, J. H. *J. Phys. Chem.* **1988**, *92*, 2346.

(13) Gu, T.; Huang, Z. *Colloids Surf.* **1989**, *40*, 71.

(14) Gao, Y.; Du, J.; Gu, T. *J. Chem. Soc., Faraday Trans. 1* **1987**, *83*, 2671.

(15) Rupprecht, H.; Gu, T. *Colloids Polym. Sci.* **1991**, *269*, 506.

is the small micelles retaining their structure but becoming more closely packed along the adsorption isotherm. On the basis of the two-step adsorption model, a general adsorption isotherm equation was also derived.¹⁶ This model was later modified to allow for different aggregation numbers for the surface micelles, and this resulted in a BET type of equation.¹⁷ The equations derived have been successfully applied to various types of adsorption isotherms for a relatively large number of systems, with the majority of studies being concerned with silica surfaces.¹³⁻¹⁷ However, there is a lack of direct experimental evidence for the formation of small micelles on the solid surface.

In order to simplify the terminology, the term "solloid"¹⁸ was created as a general term for surface *colloids* that include all sorts of adsorbed surfactant layer structures such as bilayers, monolayers, admicelles, hemimicelles, and small surface micelles. Also, modern self-consistent field lattice theory (SCFA theory) was utilized by Böhmer and Koopal in recent years to resolve theoretical controversies.^{4,5,19} SCFA theory does not require any assumptions about the adsorbed layer structure. Results obtained with the SCFA theory show the shape of the isotherm to be quite complex and different for constant charge and constant potential (variable charge) surfaces. For metal oxides, their surface potentials are about constant at a given pH.² The isotherms calculated for constant potential surfaces, plotted on a log-log scale, show the characteristic four-region behavior. At constant charge surfaces and low ionic strengths, the calculated isotherm corresponds well with the two-step isotherms found for carbon black,²⁰ biotite and fluorite,²¹ polystyrene latex,²² PTFE latex,²³ and some surfactant isotherms on silica.^{14,24-27}

According to the SCFA theory, the four-region model and the two-step model coexist and are valid under different conditions, depending on the charge properties of the solid surface. The adsorption behaviors of anionic and cationic surfactants on oppositely charged rutile were found to be the same with the isotherm shape consisting of four regions, as predicted by the SCFA theory.²⁸

Alumina is often used as a substrate for the adsorption of anionic surfactants, where four-region isotherms have been found. In the present study, the adsorption of cationic surfactants, alkyltrimethylammonium bromides (alkyl TABs), on negatively charged alumina is investigated for comparison. The study was carried through the measurements of adsorption isotherms, vacuum flotation, ESR, and fluorescence in order to fully understand the adsorption process.

2. Materials and Methods

Alumina. Linde A alumina from Union Carbide specified to be 90% α -Al₂O₃ and 10% γ -Al₂O₃ with a mean diameter of 0.3 μ m was used as the substrate for adsorption. The specific surface

(16) Zhu, B.-Y.; Gu, T. *Adv. Colloid Interface Sci.* **1991**, *37*, 1.

(17) Gu, T.; Rupprecht, H.; Galera-Gómez, P. A. *Colloid Polym. Sci.* **1993**, *271*, 799.

(18) Somasundaran, P.; Kunjappu, J. T. *Colloids Surf.* **1989**, *37*, 245.

(19) Böhmer, M. R.; Koopal, L. K. *Langmuir* **1992**, *8*, 1594.

(20) Day, R. E.; Greenwood, F. G.; Parfitt, G. D. In *Proceedings, 4th International Congress Surface Active Substances*; Gordon & Breach: London, 1967; Vol. 2B, p 1005.

(21) Cases, J. M.; Villèras, F. *Langmuir* **1992**, *8*, 1251.

(22) Connor, P.; Ottewill, R. H. *J. Colloid Interface Sci.* **1971**, *37*, 642.

(23) Bee, H. E.; Ottewill, R. H.; Rance, D. G.; Richardson, R. A. In *Adsorption from Solutions*; Ottewill, R. H., Rochester, C. H., Smith, A. L., Eds.; Academic Press: London, 1983; p 155.

(24) Ball, B.; Fuerstenau, D. W. *Discuss. Faraday Soc.* **1971**, *52*, 361.

(25) Rupprecht, H.; Ullmann, E.; Thoma, K. *Fortschr. Kolloid. Polym.* **1971**, *55*, 45.

(26) Rupprecht, H. *J. Pharm. Sci.* **1972**, *61*, 700.

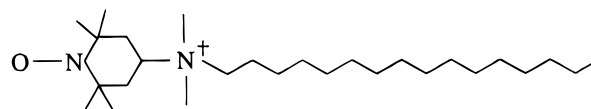
(27) Bijsterbosch, B. H. *J. Colloid Interface Sci.* **1974**, *47*, 186.

(28) Koopal, L. K.; Lee, E. M.; Böhmer, M. R. *J. Colloid Interface Sci.* **1995**, *170*, 85.

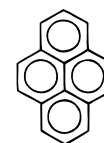
area as measured by the BET technique using nitrogen adsorption on a Quantasorb system was 15 m²/g.

Surfactants. TTAB, [CH₃(CH₂)₁₃N(CH₃)₃]Br, and DTAB, [CH₃(CH₂)₁₁N(CH₃)₃]Br, were from American Tokyo Kasei, Inc., and CTAB, [CH₃(CH₂)₁₅N(CH₃)₃]Br, was from Fluka. All the surfactants were used as received without further purification.

Probes. ESR probe CAT-16 is purchased from Molecular Probes; fluorescence probe pyrene is from Aldrich. The probes were used without further purification.



CAT-16



Pyrene

Adsorption. Adsorption experiments were conducted in capped 20 mL vials. Two-gram samples of alumina were mixed with 10 mL of 0.03 M NaCl aqueous solutions for 1 h at room temperature. The pH was adjusted as desired and the suspension allowed to equilibrate further for 1 h. Then 10 mL of 0.03 M NaCl solutions containing the surfactant at different concentrations were added, and the samples were equilibrated overnight. The pH was adjusted again using 0.1 M NaOH. The samples were equilibrated for about 3 more hours and then centrifuged for 25 min at 5000 rpm. The supernatant was then pipetted out for analysis. Surfactant concentration was determined by a two-phase titration technique,²⁹ using chloroform as the organic solvent and bromophenol blue as the indicator.

Solution Conditions. All experiments were conducted at an ionic strength of 0.03 M NaCl and at a pH of 10.0 \pm 0.3. Triply distilled water of conductivity (1-2) \times 10⁻⁶ Ω ⁻¹ was used for preparing all solutions.

Vacuum Flotation. The procedures for adsorption as described above were followed except that the amount of all the reagents were doubled so that 40 mL vials could be used. The vials were directly connected to the vacuum system (FTS systems, Inc.), the flow rate was controlled manually, stirring done using a magnetic stirrer bar, and flotation was conducted for 5 min.

ESR Measurements. ESR spectra were obtained using a Bruker EPR300 spectrometer at room temperature. CAT-16 was used as the spin probe.

Fluorescence Measurements. All fluorescence spectra were recorded on a Photon International PTI-LS 100 spectrometer. In the case of slurry samples, the fluorescence experiment was conducted in a 1 cm square and 2 mm flat quartz cell. Pyrene stock solutions were prepared by stirring pyrene in concentrated surfactant solutions for 24 h and filtering off the excess probe. Pyrene concentrations before and after adsorption were measured by UV absorbance using an extinction coefficient of 4.5 \times 10⁴ M⁻¹ cm⁻¹.

3. Results and Discussion

(1) Adsorption Isotherm Measurement. A visual examination of the adsorption isotherms of the three cationic surfactants on alumina, given in Figure 2, suggests that they do not fall into the four-region type. Specifically region III seems to be absent. However, from the shape of the isotherms alone, it is difficult to determine the real mechanisms controlling the adsorption in these systems.

The shape of a surfactant adsorption isotherm depends to a great extent on its critical micelle concentration (cmc) and critical hemimicelle concentration (hmc) which mark

(29) Li, Z.; Rosen, M. J. *Anal. Chem.* **1981**, *53*, 1516.

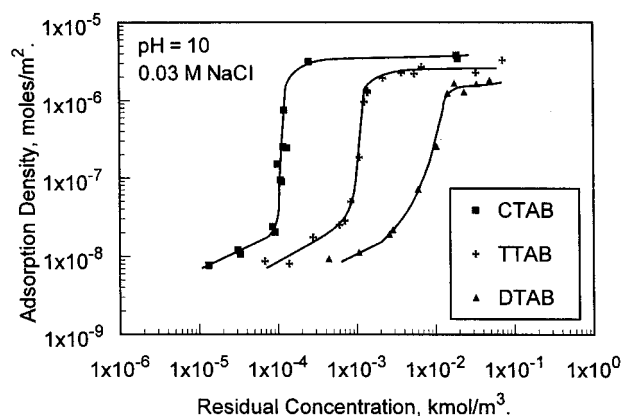


Figure 2. Adsorption isotherms for alkyltrimethylammonium bromides (CTAB, TTAB and DTAB) on alumina.

the onsets of regions II and IV, respectively. An increase in chain length is considered to decrease the Gibbs free energies of the micellization and hemimicellization processes resulting in a shift of cmc and hmc toward lower concentrations. Addition of a CH_2 group to the chain is known to decrease the cmc and hmc by a factor of 3 (Traube's rule). The experimental results presented in Figure 2 exhibit such decreases well.

Assuming the same solloid structure at the plateau region, the plateau value reflects the tightness of the packing of the solloids. For alkyl TABs adsorption on alumina, the adsorption density in the plateau region is about $(2-3) \times 10^{-6} \text{ mol/m}^2$. This value is lower than the $6.5 \times 10^{-6} \text{ mol/m}^2$ for sodium dodecyl sulfate adsorption on the same kind of alumina at pH 6.5 in 0.1 M NaCl solution.^{6,7} Three factors are proposed to contribute to this difference. First, the head group area of alkyl TAB (about 37 \AA^2) is larger than that of SDS (about 25 \AA^2). Secondly, alumina particles have a lower charge density at pH 10 (about -30 mV) than at pH 6.5 (about 40 mV). Finally, 0.1 M NaCl used for SDS adsorption is more effective in reducing head group repulsion than 0.03 M NaCl used for alkyl TAB adsorption. These three factors can all result in a tighter packing of SDS; it can be concluded that alkyl TAB solloid layers on alumina are relatively loosely packed compared to SDS solloids on alumina.

The slopes of region II and plateau values of region IV increase slightly with chain length, which is due to the increase in hydrophobic attraction upon increasing the chain length.

The stronger coherence of longer chain length was also found for $C_n\text{TAB}$ series of molecules at air/water interface by neutron reflection, which compensates the increasing tilting with longer chains and results in a lack of variation of the adsorption layer thickness with chain length.³⁰

(2) Vacuum Flotation. Flotation technique³¹ is a convenient method for determining the hydrophobicity of particles. In this technique, particles in a suspension are allowed to collide with bubbles. Particles which attach to bubbles because of their hydrophobicity will levitate to the top of the container where they can be separated and measured. The floated fraction can be used as a measure of the hydrophobicity of the particles.

In this experiment, vacuum flotation, in which bubbles are generated through the application of vacuum, was used to monitor changes in the hydrophobicity of surfac-

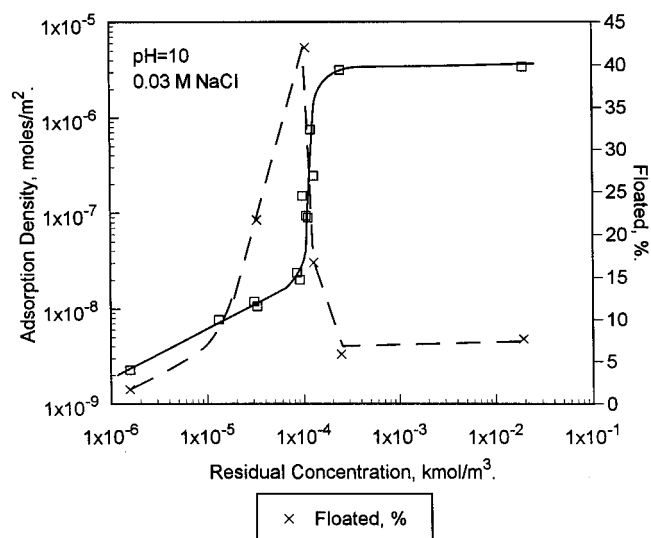


Figure 3. Correlation of alumina flotation with the adsorption isotherm of cetyltrimethylammonium bromide (CTAB).

tant-coated alumina particles along the adsorption isotherm, and the results obtained are shown in Figure 3.

Increase in flotation is considered to be due to the hydrophobicity imparted to the mineral surface by surfactant adsorption, while the decrease at higher surfactant concentrations can be due to surfactant adsorption in this range with a reverse orientation as well as to mutual repulsion between the bubbles and the particles.³² On the basis of the four-region model, flotation is expected to exhibit a maximum at the transition point between regions II and III. A maximum in Figure 3 does exist somewhere on the sharp rising portion of the isotherm. The existence of region III in the present system can hence be concluded on the basis of flotation experiments.

The difficulty in detecting region III in the isotherm is therefore proposed to result from the similarity of the slopes of regions II and III. According to the original four-region model, region III should have a smaller slope than region II. In region II, adsorption is favored both by the strong electrostatic interaction between the head group and the solid surface and the hydrophobic attraction between the tails. In region III, only the latter attraction exists with electrostatic repulsion building up as adsorption continues. For the current system, the transition between regions II and III is not perceptible on a conventional isotherm, which implies the presence of similar forces for adsorption in these regions. To account for this, the hydrophobic attraction in region III is proposed to be much stronger than that in region II so as to offset the electrostatic attraction in region II. A penetrating architecture with head-in and head-out orientations in the adsorption layers, resulting in a strong hydrophobic interaction in region III, is proposed toward this purpose. The loose structure of the solloid, the bulky head of the surfactants, and the moderate charge density of alumina at pH 10 all justify such a hypothesis.

The phenomenon of a weak or merged II/III transition was observed also in the case of dodecylpyridinium chloride/rutile adsorption when the solution pH was close to its point of zero charge (pzc).²⁸ In view of the above discussion, the proximity of pH to its pzc results in a weak electrostatic attraction in adsorption region II. Closer the pH value is to the pzc, smaller is the difference between the driving forces for adsorption in regions II and III, and hence weaker is the II/III transition.

(30) Lyttle, D. J.; Lu, J. R.; Su, T. J.; Thomas, R. K. *Langmuir* **1995**, *11*, 1001.

(31) Wills, B. A. In *Mineral Processing Technology*, 5th ed.; Pergamon Press: New York, 1992; Chapter 12, p 491.

(32) Somasundaran, P.; Chandar, P.; Chari, K. *Colloids Surf.* **1983**, *8*, 121.

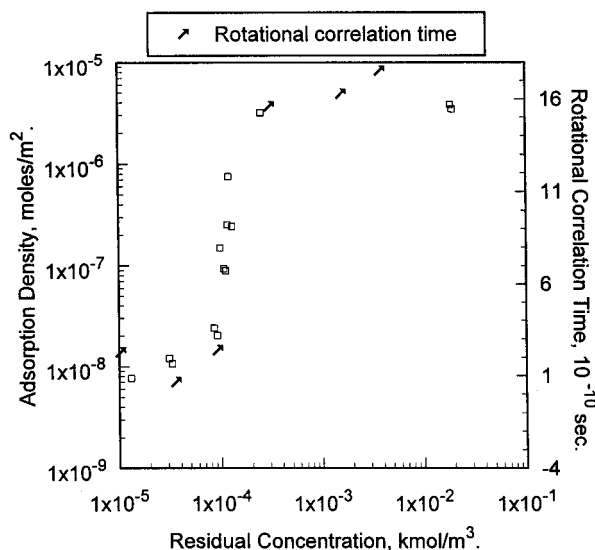


Figure 4. Rotational correlation time of CAT-16 in cetyltrimethylammonium bromide (CTAB) solloid layer along with the corresponding adsorption isotherm.

From the flotation results, a process similar to what was proposed in the four-region model can be expected to occur in the present case. Surface micelle model and bilayer model warrant continuous increase or decrease in hydrophobicity along the entire adsorption isotherm. Since such a continuous change is not observed here, they can both be excluded for the current system. On the basis of the above results, a loose and interpenetrating configuration for the solloid layer is suggested for the system under study.

(3) ESR Results. The ESR spectra of CAT-16 were used to determine changes in environmental polarity and viscosity of solloids along the adsorption isotherms. Contributions from probe in the bulk solutions to the ESR signal intensities are negligible in all cases. The measurable parameters from these spectra include the nitrogen hyperfine splitting constant, A_N , and the rotational correlation time, τ_C .

The nitrogen hyperfine splitting constant can be obtained from the average separation of the three lines of the ESR spectrum. Since A_N does decrease with micropolarity decrease, it is a good measure of the micropolarity of the probe environment. ESR spectrum becomes increasingly anisotropic as the solvent viscosity increases as a result of the decrease in rotational mobility of the probe. The rotational correlation times can be calculated from³³

$$\tau_C \text{ (s)} = 6.5 \times 10^{-10} \Delta H [(h_0/h_{-1})^{1/2} - 1]$$

where ΔH is the peak to peak width of the central line. h_0 and h_{-1} are the heights of the central and high field lines, respectively. Thus, τ_C provides a direct measurement of the microviscosity of the probe environment. Figures 4–6 show τ_C values of the ESR spectra obtained for the alumina in CTAB, TTAB, and DTAB solutions, respectively, with isotherms also plotted in the same figure for comparison purposes. It can be seen that rotational correlation time plots correlate with the adsorption isotherms so well that they almost overlap. It is clear that the rotation of the probe molecule is severely restricted in the solloid layers as expected. The hyperfine splitting

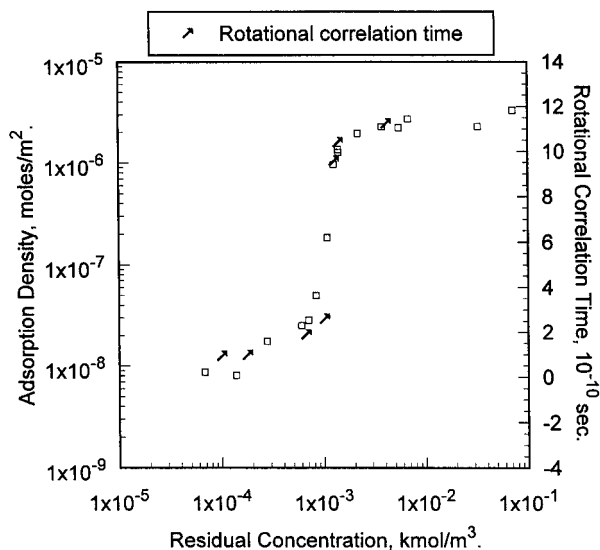


Figure 5. Rotational correlation time of CAT-16 in tetradecyltrimethylammonium bromide (TTAB) solloid layer along with the corresponding adsorption isotherm.

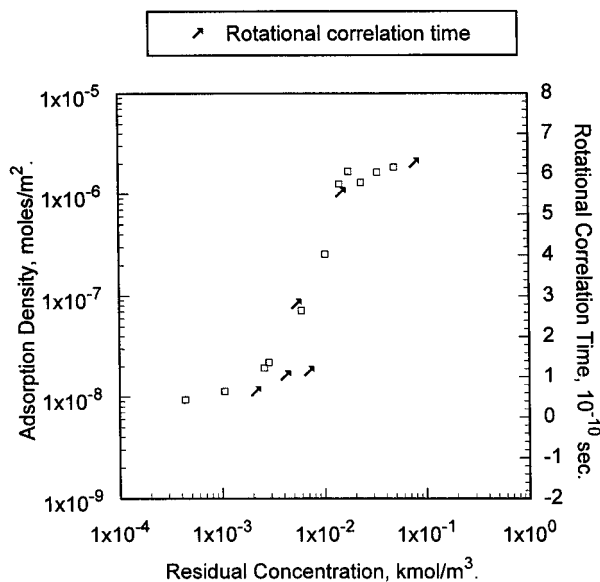


Figure 6. Rotational correlation time of CAT-16 in dodecyltrimethylammonium bromide (DTAB) solloid layer along with the corresponding adsorption isotherm.

constant is found to decrease upon solloid formation on the surface (Figure 7), indicating a more hydrophobic environment for the probe.

It can be seen from Figure 8 that the plateau values of rotational correlation times vary significantly with surfactant chain length. Probes in CTAB solloids are most restricted, whereas those in DTAB solloids are most mobile. The chain length of the probe molecule is the same as that of CTAB and longer than those of TTAB and DTAB. Thus the shorter the host chain length, the higher the freedom of the nitroxide group of the probe in adsorbed layer of the surfactant.

(4) Fluorescence Decay of Pyrene in the Adsorbed Layer. The principles for determination of micelle aggregation number from data for fluorescence decay have been reviewed extensively elsewhere.^{34,35} However, the technique has rarely been used to obtain solloid aggrega-

(33) Knowles, P. F.; Marsh, D.; Rattle, H. W. E. In *Magnetic Resonance of Biomolecules: An Introduction to the Theory and Practice of NMR and ESR in Biological Systems*; John Wiley & Sons: New York, 1976.

(34) Zana, R. In *Surfactant Solutions*; Zana, R., Ed. Surfactant Science Series, Vol. 22; Marcel Dekker: New York, 1987; p 241.

(35) Zana, R.; Yiv, S.; Strazielle, C.; Lianos, P. *J. Colloid Interface Sci.* **1981**, *80*, 208.

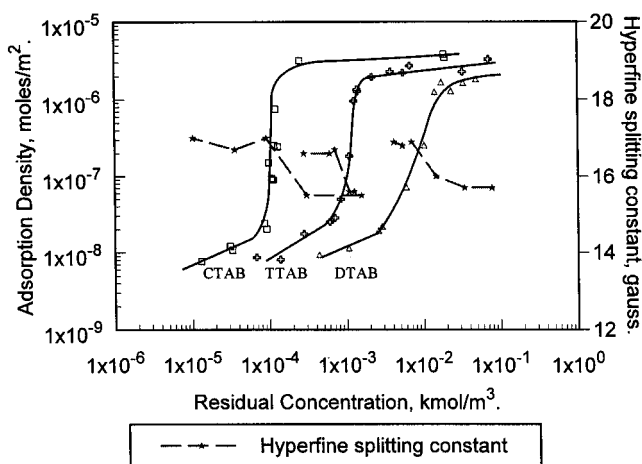


Figure 7. Hyperfine splitting constants of CAT-16 in alkyltrimethylammonium bromide solloid layers along with the corresponding adsorption isotherms.

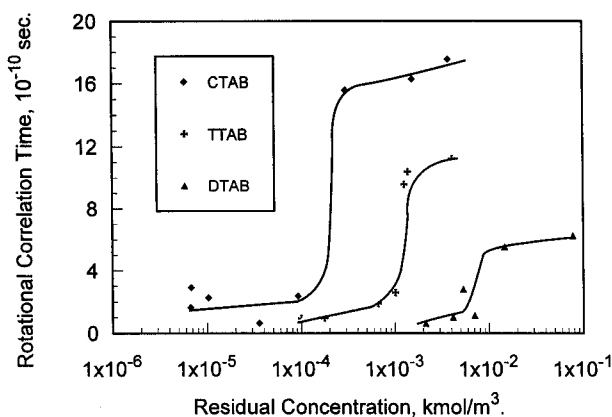


Figure 8. Rotational correlation times of CAT-16 in solloid layers of alkyl TABs of three different chain lengths.

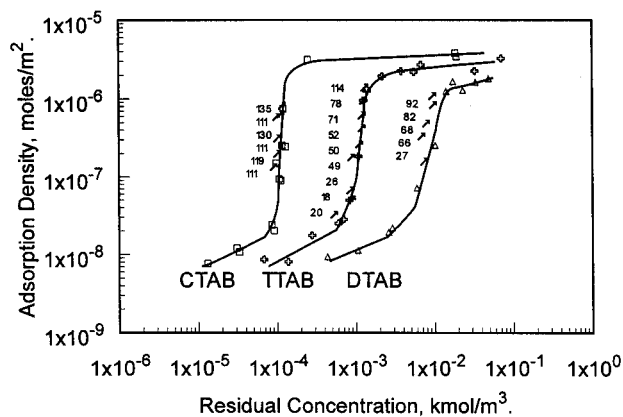


Figure 9. Aggregation numbers for alkyltrimethylammonium bromide solloids of three different chain lengths on alumina.

tion numbers on metal oxides.⁷ The solloid aggregation numbers obtained in the current study are presented in Figure 9, which shows a change in aggregate size along the rising part of TTAB and part of the sharp rising parts of CTAB and DTAB isotherms. The average aggregation numbers, N , measured at particular adsorption densities are indicated along the isotherm. It is to be noted that at all concentrations under study, no pyrene was detected in the supernatant of each sample.

In general, the size of aggregate can be seen to increase with adsorption density. In the middle range of the sharp increase in the isotherm, the aggregation number stays

constant as in region II of the four-region model. In the upper range of the sharp increase, there is a significant increase in the aggregation number, as in region III of the four-region model. The increase in solloid size with chain length is also to be noted. It is helpful to compare the above results with results obtained previously for the sodium dodecyl sulfonate (SDS)/alumina system:⁷

(1) The probe induces a slight increase in the adsorption of the surfactant. However, for all the systems studied, the change in adsorption upon probe addition can be considered to be insignificant.

(2) A similar trend of N value increase was found for both system (N values of 66, 49, 121, 123, 128, 166, 196, 258, and 356 were found for SDS solloids⁷ and those of 20, 18, 26, 49, 50, 52, 71, 78, and 114 were found for TTAB solloids as shown in Figure 9). In the initial stage of region II, the aggregation number is quite small in both cases. These aggregates grow from monomers in region I and apparently serve as big hydrophobic anchors for further adsorption. It is evident that further adsorption results in an almost constant solloid size at the end of region II. This stage of region II where N is constant indicates a process similar to micellization. It is to be noted that these constant N values are about the same as their micelle aggregation numbers. However, the solloid structure has to be different from the micelle structure. There has to be more head-on adsorption than head-out adsorption, which makes further adsorption in region III and a maximum in flotation possible.

(3) The N values for SDS solloids are considerably larger than those for alkyltrimethylammonium bromide of the same chain length, although the trend is almost the same. This is consistent with the higher plateau value of SDS adsorption. It can also be seen that N increases with the chain length. The slight increase in both slope and plateau values with chain length are in accord with this observation.

From the fluorescence study, a four-region model is once again supported. It was also found that the looser structure of solloid, the lower plateau value of the adsorption isotherm, and the smaller solloid aggregation number are all closely related to one another. In addition, solloid grows in size in the initial part of region II without much size change in the later stage of region II.

4. Conclusions

From the results obtained for adsorption isotherm, flotation, ESR, and fluorescence, it can be concluded that the adsorption mechanism for alkyltrimethylammonium bromides on alumina is in accord with the four-region model, although only three regions were detected on the conventional adsorption isotherms; this is suggested to be the result of a loose and interpenetrating configuration of the solloids. The results suggest that the solloid nature, as a dominating factor in deciding the shape of adsorption isotherm, is influenced greatly by the type of surfactant, the solid, and solution conditions.

Acknowledgment. The authors acknowledge the support of the National Science Foundation.